The efficiency of Raman amplification in the wavebreaking regime

Matthew R. Edwards,[1,a)] Zeev Toroker,[2] Julia M. Mikhailova,[1,b)] and Nathaniel J. Fisch[3]
[1]*Department of Mechanical and Aerospace Engineering, Princeton University, Princeton, New Jersey 08544, USA*
[2]*Department of Electrical Engineering, Technion Israel Institute of Technology, Haifa 32000, Israel*
[3]*Department of Astrophysical Sciences, Princeton University, Princeton, New Jersey 08544, USA*

(Received 13 April 2015; accepted 19 June 2015; published online 15 July 2015)

We compare previous analytic predictions, Vlasov-Maxwell simulations, and particle-in-cell results with a new set of comprehensive one and two dimensional particle-in-cell simulations in an effort to clarify apparent discrepancies between the predictions of different models for the efficiency of Raman amplification in the wavebreaking regime. We find reasonable agreement between our particle-in-cell simulations and previous results from Vlasov-Maxwell simulations and analytic work, suggesting a monotonic decrease in conversion efficiency for increased pump intensities past the wavebreaking threshold. © *2015 AIP Publishing LLC*. [http://dx.doi.org/10.1063/1.4926514]

Backward Raman amplification (BRA) of short laser pulses in plasmas[1] provides a possible method to avoid the intensity limit of the final compression grating in chirped pulse amplification (CPA) systems.[2,3] BRA utilizes the resonant three-wave interaction between a Langmuir wave (at frequency ω_e), a long pump laser (at frequency ω_a), and a downshifted short seed laser (at frequency $\omega_b = \omega_a - \omega_e$) to transfer energy from the pump to the seed, producing a short intense pulse. In principle, intensities of 10^{17} W/cm^2 can be reached for optical-regime beams,[4] with up to 4×10^{16} W/cm^2 (Ref. 5) demonstrated experimentally.[6–17]

In addition to the frequency matching (energy conservation) condition, BRA requires that the wavevectors of the two lasers and the plasma wave satisfy momentum conservation: $\mathbf{k}_a = \mathbf{k}_b + \mathbf{k}_e$. The efficiency of BRA may be limited by relativistic nonlinearities,[1,4,18–22] spontaneous Raman scattering,[1,4,23–26] Landau damping of the Langmuir wave,[17,19,27–32] wavebreaking,[1,4] inverse bremsstrahlung,[19,29,33,34] and plasma inhomogeneities.[35] Of particular interest for the development of Raman amplification systems are parameter regimes which provide increased conversion efficiencies while avoiding instabilities, especially regimes which are robust to small variations in parameters.[36–39]

In this note, we consider amplification beyond the wavebreaking threshold, a limitation on the efficiency of Raman amplification set by the breakup of the Langmuir wave when the electron longitudinal quiver velocity exceeds the plasma-wave phase velocity. Initial study of Raman amplification predicted that conversion efficiency would increase until the wavebreaking threshold, after which further increases in pump intensity would result in rapidly decreasing efficiency.[1] More recent particle-in-cell (PIC) simulations have suggested that a narrow parameter window exists in the strong wavebreaking regime where amplification efficiency reaches 35%.[40] This is much higher than the efficiencies expected at those parameters from approximate analytic results[1] (≈5%) and later simulations with a Vlasov-Maxwell code[41] (≈10%). A high-efficiency region in the strong wavebreaking regime might allow faster seed growth and decreased sensitivity to parasitic Raman forward scattering,[41] making operation beyond the wavebreaking threshold advantageous. A strong motivation therefore exists to accurately characterize the behavior of Raman amplification in this regime. In view of the discrepancies between predictions of different models in this potentially useful regime, we use a PIC code different from that in Ref. 40 to generate a comprehensive set of simulations in the wavebreaking regime for comparison and verification of previous results.

The degree of wavebreaking can be described by $\bar{v}_{ea}/\bar{v}_{br}$, where $\bar{v}_{ea} = E_a e/m_e \omega_a c$ is the normalized longitudinal electron quiver velocity and $\bar{v}_{br} = (2\omega_a/\omega_e)^{-3/2}$ is the quiver velocity at the wavebreaking threshold. The wavebreaking regime is reached for $\bar{v}_{ea}/\bar{v}_{br} > 1$. For a plasma with density 4.5×10^{18} cm^{-3} ($n_e = 0.0026 n_c$, where n_c is the critical density) and a pump laser with wavelength 800 nm, the corresponding wavebreaking threshold intensity is 3.5×10^{13} W/cm^2 and $\bar{v}_{br}$ is 0.004. Under these conditions, the seed wavelength required for phase matching is 843 nm and $k_e \lambda_{De} = 0.17$, where λ_{De} is the Debye length and k_e is the wavenumber of the Langmuir wave.

Some care needs to be taken with calculations of efficiency, due to its importance as a metric and the different methods which have been used in the literature. The final energy of the seed laser may be compared to the total energy in the pump laser, as in Ref. 40

$$\eta_W = \frac{W_{\text{seed},f}}{W_{\text{pump},0}}, \tag{1}$$

where W is the total electromagnetic energy in the seed or pump initially (0) or after the plasma interaction (f). This formula is adequate when the initial energy in the seed is small compared to the final energy in the seed, but must be modified when the initial seed is much more intense than the initial pump to account for the initial seed energy

[a)]Electronic address: mredward@princeton.edu
[b)]Electronic address: jm41@princeton.edu

$$\eta_W = \frac{W_{\text{seed},f} - W_{\text{seed},0}}{W_{\text{pump},0}}. \quad (2)$$

A second method to calculate efficiency, as used in Ref. 41, compares the initial pump intensity to the pump intensity at some specific location behind the seed front

$$\eta_I = \frac{I_{\text{pump},f}}{I_{\text{pump},0}}. \quad (3)$$

The above two methods of calculating efficiency will give slightly different results. First, η_I counts all energy that leaves the pump as converted, whereas η_W considers only energy that arrives in the seed. Since some energy is lost to the plasma, η_I will be higher than η_W. Second, as previously calculated,[40,41] η_W is an average over the entire interaction, but η_I only compares the initial and final pump intensities at a single time. If the pump depletion is the same throughout the entire interaction, this will not make a difference, but under many conditions, the pump is increasingly depleted as the seed progresses. A calculation of η_I at the end of the simulation will therefore tend to produce a higher value than one for η_W. Depending on how the calculations are actually implemented, these two methods may also account for spontaneous Raman backscattering differently. In general, η_I will be slightly higher than η_W; though for the conditions presented here, we will show that the difference is small and does not significantly affect the results.

The new PIC simulations presented in this paper were run with the code EPOCH in a fixed frame without a moving window. One dimensional simulations were conducted with 25 cells per wavelength and 16 particles per cell, where $\lambda = 800$ nm is the pump laser wavelength. The two dimensional simulations used resolutions of $\Delta x/\lambda = 0.1$ (longitudinal) and $\Delta y/\lambda = 0.1$ (transverse), with one particle per cell. Unless otherwise noted, the electron temperature was 10 eV, and ions were always left immobile. The one-dimensional simulations were conducted in a plasma of length 4 mm, and the two-dimensional simulations were conducted in a 1.3 mm plasma.

Figure 1(a) compares analytic predictions from Ref. 1 and Vlasov-Maxwell simulations from Ref. 41 with one and two dimensional PIC simulations conducted with the code EPOCH. The analytic model predicts that the efficiency drops with $(\bar{v}_{ea}/\bar{v}_{br})^2$, a trend which is closely followed by the Vlasov-Maxwell results for moderate wavebreaking, and approximately followed by the PIC results, though both the Vlasov-Maxwell and PIC simulations suggest higher intensities than the analytic results for these seed intensities in the strong wavebreaking regime. As a comparison to previous results,[40,41] we have provided both η_W and η_I for the one dimensional PIC simulations, though, as shown in Figure 1, the difference between the two efficiency measures is not large in the wavebreaking regime. This agreement results from relatively steady pump depletion in this regime. The two dimensional result at $\bar{v}_{ea}/\bar{v}_{br} = 7.5$ is meant to replicate the conditions at which 35% efficiency was found in Ref. 40 as closely as possible. Note that due to transverse variation in pump and probe intensities, the corresponding value of

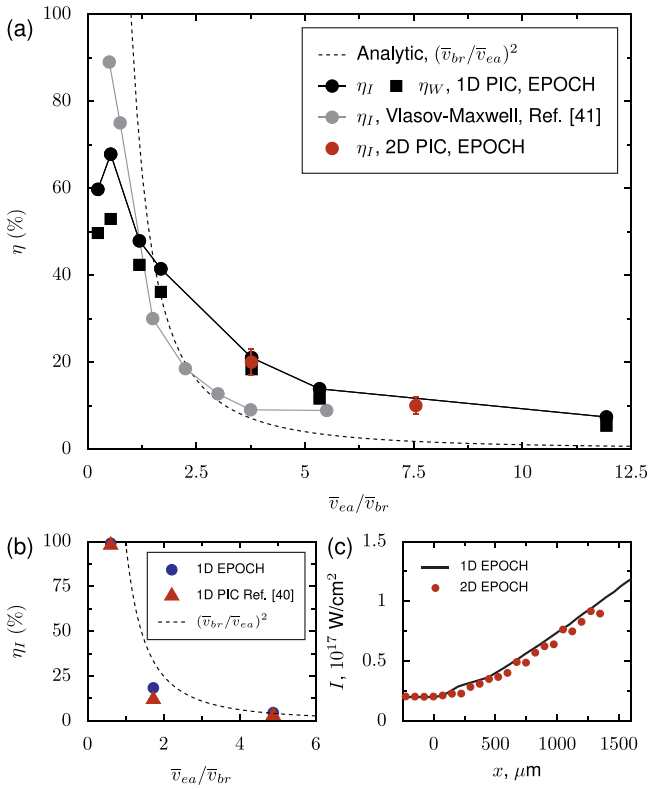

FIG. 1. Efficiency of Raman amplification in the wavebreaking regime. (a) Comparison of analytic predication with Vlasov-Maxwell simulations (from Ref. 41) and 1D and 2D PIC simulations. The one-dimensional simulations use an initial seed intensity of 10^{16} W/cm^2. The two-dimensional simulations have an initial centerline seed intensity of 2×10^{16} W/cm^2. (b) Comparison of one-dimensional simulations in Ref. 40 (Figure 3(a)) and the current work, where the initial seed intensity is 10^{15} W/cm^2, the pump intensity is 10^{14} W/cm^2, and ω_a/ω_e is varied. The points correspond to $\omega_a/\omega_e = 10$, 20, and 40. The value of η_I from Ref. 40 is estimated from the steady state value of the depleted pump intensity, extracted from a plot of the pump intensity as a function of distance. (c) Increase in intensity of seed pulse for one and two dimensional simulations with $I_{\text{pump},0} = 2 \times 10^{15}$ W/cm^2, $\bar{v}_{ea}/\bar{v}_{br} = 7.5$, and $I_{\text{seed},0} = 2 \times 10^{16}$ W/cm^2. The values presented for the two dimensional simulation are calculated at the centerline.

$\bar{v}_{ea}/\bar{v}_{br}$ may change depending on whether the centerline intensity (as is done here) or FWHM intensity (Ref. 41) is used. Here, we have chosen to use the centerline value for ease of comparison to one-dimensional results and because of the importance of peak intensity in discussing amplification. The initial centerline pump intensity (2×10^{15} W/cm^2), seed intensity (2×10^{16} W/cm^2), and plasma density (4.5×10^{18} cm^{-3}) are the same, though the spatial full-width-half-maximum (FWHM) of the beam is smaller (140 μm vs 700 μm in Ref. 40). The error bars for the two dimensional results represent differences in efficiency found depending on how much of the width of the beam is included in the calculation.

In Figure 1(b), calculations of η_I using one-dimensional simulations are compared to previous simulations presented in Fig. 3 of Ref. 40 at varied ω_a/ω_e. The initial pump and seed intensities are 10^{14} and 10^{15} W/cm^2, respectively. The two different sets of PIC simulations agree with the previous analytic and Vlasov-Maxwell results, suggesting that the previous models have well-captured the fundamental dynamics of this regime, at least in one dimension. These results are

somewhat different from those found when the pump intensity is varied instead of the plasma density, due in part to the different rates at which maximum depletion is reached for different densities and in part to the lower pump and seed intensities providing a better match to the analytic assumptions.

The appropriateness of one-dimensional simulations in analyzing the first-order behavior of Raman amplification may be assessed by directly comparing the centerline of a two dimensional simulation to a one dimensional simulation under similar conditions. In Figure 1(c), the centerline seed intensity of the two dimensional PIC simulation corresponding to the point at $\bar{v}_{ea}/\bar{v}_{br} = 7.5$ in Figure 1(a) is compared to a one dimensional PIC simulation at the centerline conditions. The agreement between the one-dimensional and two-dimensional simulations, which should be worse for narrow beams and low resolution, suggests that those factors do not substantially affect the efficiency of Raman amplification in the wavebreaking regime.

To check against possible sensitivity of the observed efficiency to small variations in seed or pump intensities, we used one-dimensional PIC simulations to calculate η_I for different initial pump (through $\bar{v}_{ea}/\bar{v}_{br}$) and seed intensities (Figure 2). Although the efficiency increases with seed intensity, it does not appear that any reasonable increase in seed intensity can produce 35% efficiency in the strong-wavebreaking regime. It is not particularly useful to consider further increases in seed intensity (above $10^{17}\,\mathrm{W/cm^2}$) due to the longitudinal and transverse modulation instabilities that develop for relativistic seed laser intensities, making BRA unsuitable for further amplification. At low seed intensities, the efficiency appears to approach the analytic result, as would be expected based on the neglect of the seed intensity in the analytic model.[1] The improved efficiency at increased seed intensity appears similar to the behavior of BRA in the quasi-transient regime, where the Langmuir wave is Landau damped,[29,33,34] possibly allowing the analytic tools developed to describe the quasi-transient regime to be applied to the wavebreaking regime. As higher seed intensities are employed, we may also approach the regime of super-radiant amplification by Compton backscattering.[42] This regime occurs when $\omega_B > \omega_e$, where $\omega_B = \omega_a\sqrt{2\bar{v}_{ea}\bar{v}_{eb}}$ is the electron bounce frequency associated with the ponderomotive force in the beat wave of the two lasers for linear polarization.[43] For $\omega_a/\omega_e = 20$ and initial pump and seed intensities of $10^{15}\,\mathrm{W/cm^2}$, we already have $\omega_B = 0.6\omega_e$.

Since all of the analysis considered here assumes immobile ions, the plasma is entirely described by electron density and temperature. The effect of plasma density is well captured by its inclusion in $\bar{v}_{ea}/\bar{v}_{br}$, as shown by Figure 1(b), where the simple analytic model predicts efficiency variation for different plasma densities. Figure 3 illustrates the effect of variation in electron temperature on the Raman amplification growth rate of a seed with initial intensity of $10^{16}\,\mathrm{W/cm^2}$, in a $10^{15}\,\mathrm{W/cm^2}$ pump and 4.5×10^{18} $\mathrm{cm^{-3}}$ density plasma, which corresponds to $\bar{v}_{ea}/\bar{v}_{br} = 5.5$. Initially, lower temperatures produce higher growth rates, but over longer propagation distances, growth at higher temperatures is greater, perhaps, because less of the pump is depleted by spontaneous Raman scattering. Overall, the effect of electron temperature is small, causing no more than a 25% difference in final seed intensity. We note that across our simulations energy is conserved, with the Manley-Rowe relations satisfied even for strong wavebreaking, and there is no significant spontaneous heating of the plasma.

We have extended theoretical analysis of BRA efficiency in the wavebreaking regime using new one- and two-dimensional PIC simulations. The above results eliminate several possible causes for previous disagreements in predicted BRA efficiency in the wavebreaking regime, but have not yet established a definitive explanation for them. The verification of previous Vlasov-Maxwell[41] and analytic[1] predictions by the current set of PIC results paints a consistent picture of BRA beyond the wavebreaking threshold in one dimension, with efficiency decreasing monotonically.

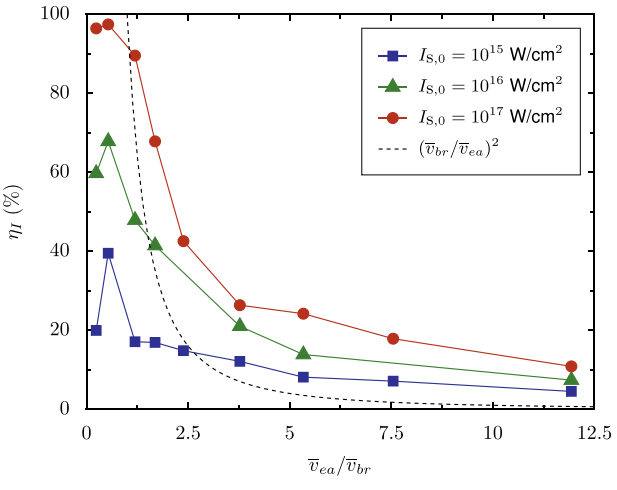

FIG. 2. Efficiency (η_I) of Raman amplification for varied seed and pump intensity. The plasma is 4 mm long and has a density of 4.5×10^{18} $\mathrm{cm^{-3}}$. $\bar{v}_{ea}/\bar{v}_{br}$ is varied by changing pump intensity between 2×10^{12} and 5×10^{15} $\mathrm{W/cm^2}$.

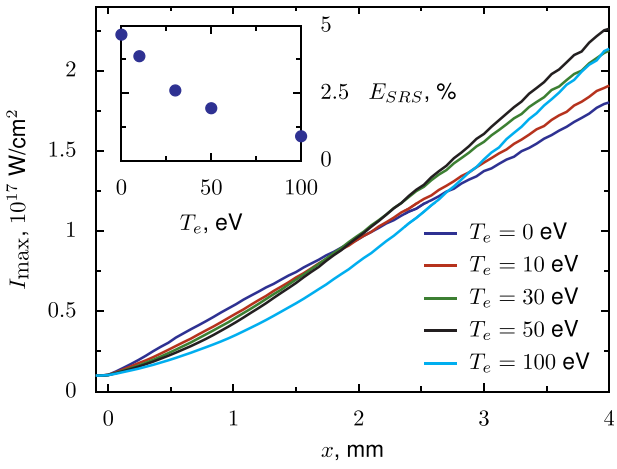

FIG. 3. Effect of initial electron temperature on Raman amplification for propagation through a 4 mm plasma with an initial pump intensity of $10^{15}\,\mathrm{W/cm^2}$. The plasma density is 4.5×10^{18} $\mathrm{cm^{-3}}$, and the initial seed intensity is $10^{16}\,\mathrm{W/cm^2}$. Inset: the energy of spontaneously Raman backscattered light (E_{SRS}) as a percentage of the incident pump energy for different plasma electron temperatures.

Our one-dimensional efficiencies respond predictably to changing initial seed intensities and are not particularly sensitive to initial temperature, ruling out the possibility that small variations in those parameters may cause large increases in efficiency. Our two-dimensional PIC results accurately recover our one-dimensional PIC findings, including the simulation matched to the physical conditions where 35% efficiency was previously found,[40] though we used a narrower beam waist (by a factor of five) for both the pump and seed. The discrepancy between previous results is therefore not likely to be a simple result of moving from one dimension to two dimensions. The long Rayleigh range of the beams in the two-dimensional simulations precludes simple beam focusing as a cause of different intensity growth, but does not rule out, for example, self-focusing effects due to the plasma, which may have been captured differently by the different beam widths and PIC implementations.

This work was supported in part by the DTRA under Grant No. HDTRA1-11-1-0037 and by the NSF under Grant No. PHY-1202162. M.R.E. was supported by an NSF Graduate Research Fellowship. These simulations were performed at the TIGRESS high performance computer center at Princeton University. The EPOCH code was developed as part of the UK EPSRC 300 360 funded Project EP/G054940/1.

[1]V. Malkin, G. Shvets, and N. Fisch, Phys. Rev. Lett. **82**, 4448 (1999).
[2]D. Strickland and G. Mourou, Opt. Commun. **55**, 447 (1985).
[3]I. V. Yakovlev, Quantum Electron. **44**, 393 (2014).
[4]V. Malkin and N. Fisch, Eur. Phys. J. Spec. Top. **223**, 1157 (2014).
[5]J. Ren, S. Li, A. Morozov, S. Suckewer, N. Yampolsky, V. Malkin, and N. Fisch, Phys. Plasmas **15**, 056702 (2008).
[6]Y. Ping, I. Geltner, N. Fisch, G. Shvets, and S. Suckewer, Phys. Rev. E **62**, R4532 (2000).
[7]Y. Ping, I. Geltner, A. Morozov, N. Fisch, and S. Suckewer, Phys. Rev. E **66**, 046401 (2002).
[8]Y. Ping, W. Cheng, S. Suckewer, D. S. Clark, and N. J. Fisch, Phys. Rev. Lett. **92**, 175007 (2004).
[9]A. A. Balakin, D. V. Kartashov, A. M. Kiselev, S. Skobelev, A. N. Stepanov, and G. M. Fraiman, J. Exp. Theor. Phys. Lett. **80**, 12 (2004).
[10]W. Cheng, Y. Avitzour, Y. Ping, S. Suckewer, N. J. Fisch, M. S. Hur, and J. S. Wurtele, Phys. Rev. Lett. **94**, 045003 (2005).
[11]R. Kirkwood, E. Dewald, C. Niemann, N. Meezan, S. Wilks, D. Price, O. Landen, J. Wurtele, A. Charman, R. Lindberg *et al.*, Phys. Plasmas **14**, 113109 (2007).
[12]C.-H. Pai, M.-W. Lin, L.-C. Ha, S.-T. Huang, Y.-C. Tsou, H.-H. Chu, J.-Y. Lin, J. Wang, and S.-Y. Chen, Phys. Rev. Lett. **101**, 065005 (2008).
[13]N. Yampolsky, N. Fisch, V. Malkin, E. Valeo, R. Lindberg, J. Wurtele, J. Ren, S. Li, A. Morozov, and S. Suckewer, Phys. Plasmas **15**, 113104 (2008).
[14]Y. Ping, R. Kirkwood, T.-L. Wang, D. Clark, S. Wilks, N. Meezan, R. Berger, J. Wurtele, N. Fisch, V. Malkin *et al.*, Phys. Plasmas **16**, 123113 (2009).
[15]D. Turnbull, S. Li, A. Morozov, and S. Suckewer, Phys. Plasmas **19**, 073103 (2012).
[16]G. Vieux, A. Lyachev, X. Yang, B. Ersfeld, J. Farmer, E. Brunetti, R. Issac, G. Raj, G. Welsh, S. Wiggins *et al.*, New J. Phys. **13**, 063042 (2011).
[17]S. Depierreux, V. Yahia, C. Goyon, G. Loisel, P.-E. Masson-Laborde, N. Borisenko, A. Orekhov, O. Rosmej, T. Rienecker, and C. Labaune, Nat. Commun. **5**, 4158 (2014).
[18]G. M. Fraiman, N. A. Yampolsky, V. M. Malkin, and N. J. Fisch, Phys. Plasmas **9**, 3617 (2002).
[19]V. Malkin and N. Fisch, Phys. Rev. Lett. **99**, 205001 (2007).
[20]V. Malkin, Z. Toroker, and N. Fisch, Phys. Plasmas **19**, 023109 (2012).
[21]G. Lehmann and K. Spatschek, Phys. Plasmas **21**, 053101 (2014).
[22]V. Malkin, Z. Toroker, and N. Fisch, Phys. Plasmas **21**, 093112 (2014).
[23]V. Malkin, G. Shvets, and N. Fisch, Phys. Plasmas **7**, 2232 (2000).
[24]V. Malkin, G. Shvets, and N. Fisch, Phys. Rev. Lett. **84**, 1208 (2000).
[25]V. Malkin, Y. A. Tsidulko, and N. Fisch, Phys. Rev. Lett. **85**, 4068 (2000).
[26]A. Solodov, V. Malkin, and N. Fisch, Phys. Rev. E **69**, 066413 (2004).
[27]M. Hur, R. Lindberg, A. Charman, J. Wurtele, and H. Suk, Phys. Rev. Lett. **95**, 115003 (2005).
[28]N. Yampolsky and N. Fisch, Phys. Plasmas **16**, 072105 (2009).
[29]V. Malkin and N. Fisch, Phys. Plasmas **17**, 073109 (2010).
[30]N. A. Yampolsky and N. J. Fisch, Phys. Plasmas **18**, 056711 (2011).
[31]D. Strozzi, E. Williams, H. Rose, D. Hinkel, A. Langdon, and J. Banks, Phys. Plasmas **19**, 112306 (2012).
[32]Z. Wu, Y. Zuo, J. Su, L. Liu, Z. Zhang, and X. Wei, IEEE Trans. Plasma Sci. **42**, 1704 (2014).
[33]V. Malkin and N. Fisch, Phys. Rev. E **80**, 046409 (2009).
[34]A. Balakin, N. Fisch, G. Fraiman, V. Malkin, and Z. Toroker, Phys. Plasmas **18**, 102311 (2011).
[35]A. Solodov, V. Malkin, and N. Fisch, Phys. Plasmas **10**, 2540 (2003).
[36]D. S. Clark and N. J. Fisch, Phys. Plasmas **10**, 3363 (2003).
[37]N. A. Yampolsky, V. Malkin, and N. Fisch, Phys. Rev. E **69**, 036401 (2004).
[38]Z. Toroker, V. Malkin, A. Balakin, G. Fraiman, and N. Fisch, Phys. Plasmas **19**, 083110 (2012).
[39]Z. Toroker, V. Malkin, and N. Fisch, Phys. Rev. Lett. **109**, 085003 (2012).
[40]R. Trines, F. Fiuza, R. Bingham, R. Fonseca, L. Silva, R. Cairns, and P. Norreys, Nat. Phys. **7**, 87 (2011).
[41]Z. Toroker, V. Malkin, and N. Fisch, Phys. Plasmas **21**, 113110 (2014).
[42]G. Shvets, N. Fisch, A. Pukhov, and J. Meyer-ter Vehn, Phys. Rev. Lett. **81**, 4879 (1998).
[43]G. Shvets, J. Wurtele, and B. Shadwick, Phys. Plasmas **4**, 1872 (1997).